TAKAGI, S. (1969). *J. Phys. Soc. Jpn*, **26**, 1239–1253.

TAUPIN, D. (1964). *Bull. Soc. Fr. Minéral. Cristallogr.* **87**, 469–511.

TEMPLETON, D. H. & TEMPLETON, L. K. (1980). *Acta Cryst.* A36, 237–241.

TEMPLETON, D. H. & TEMPLETON, L. K. (1982). *Acta Cryst.* A38, 62–67.

TEMPLETON, D. H. & TEMPLETON, L. K. (1985a). *Acta Cryst.* A41, 133–142.

TEMPLETON, D. H. & TEMPLETON, L. K. (1985b). *Acta Cryst.* A41, 365–371.

TEMPLETON, D. H. & TEMPLETON, L. K. (1987). *Acta Cryst.* A43, 573–574.

TEMPLETON, D. H. & TEMPLETON, L. K. (1988). *Acta Cryst.* A44, 1045–1051.

TEMPLETON, D. H. & TEMPLETON, L. K. (1989). *Acta Cryst.* A45, 39–42.

WAGENFELD, H. (1968). *Acta Cryst.* A24, 170–174.

WU, Y., PARKIN, S. S. P., STÖHR, J., SAMANT, M. G., HERMSMEIER, B. D., KORANDA, S., DUNHAM, D. & TONNER, B. P. (1993). *Phys. Rev. Lett.* **63**, 263–265.

Diffraction by Aggregates of Helical Molecules

BY R. P. MILLANE AND W. J. STROUD

Whistler Center for Carbohydrate Research, Purdue University, West Lafayette, IN 47907-1160, USA

(Received 3 June 1994; accepted 8 November 1994)

Abstract

An expression is derived for the intensity diffracted by a non-crystalline fiber made up of aggregates of helical molecules. This expression is useful for the efficient calculation of diffraction from such specimens and provides insight into the effects of aggregation on diffraction patterns. Example calculations show a number of implications for structure determination.

1. Introduction

X-ray fiber diffraction is used to determine the structures of polymers and other macromolecules that exist naturally as, or can be prepared as, oriented fibers or planar arrays (Millane, 1988). The molecules themselves usually adopt helical structures. In some specimens, the molecules are merely oriented with their long axes approximately parallel and are randomly rotated about these axes (Namba & Stubbs, 1985; Bhattacharjee, Glucksman & Makowski, 1992). In others, the molecules further organize laterally into very small crystalline regions and the orientations of the crystallites about the long axes of the constituent molecules are random (Leslie, Arnott, Chandrasekaran & Ratliff, 1980). These are referred to as non-crystalline and polycrystalline specimens, respectively. Specimens exhibiting ordering intermediate between these two extremes also exist (Millane & Stroud, 1991). Structure determination involves calculation of the intensity diffracted by the specimen and, in the case of a non-crystalline fiber, this is equal to the cylindrical average of the intensity of the Fourier transform of one molecule.

Other cases occur, however, where two or more helical molecules aggregate in a specific manner to form the fundamental particles that are randomly rotated in a fiber specimen. The intensity diffracted by the specimen is then related to the Fourier transform of the aggregate structure, which sometimes can be a computationally intensive calculation. The objective of this paper is to derive an expression for the intensity diffracted by such a specimen, in terms of the Fourier transform of a single molecule and the geometric relationships between the molecules. This provides a substantial decrease in the amount of computation required, compared to a calculation directly from the aggregate structure, and provides insight into differences in the diffraction by independent and by aggregated molecules.

There are a number of macromolecular systems that exhibit this kind of aggregation, for which these results might be useful, and some examples where X-ray fiber diffraction has been used to derive structural information are as follows. Nucleic acids form double- and triple-stranded molecules that are made up of two or three (almost) identical strands (Leslie, Arnott, Chandrasekaran & Ratliff, 1980; Park, Arnott, Chandrasekaran, Millane & Campagnari, 1987), and polysaccharides such as carrageenans and gellan form double helices (Millane, Chandrasekaran, Arnott & Dea, 1988; Chandrasekaran, Millane, Arnott & Atkins, 1988). Aggregates of polysaccharide helices formed by lateral associations have also been considered (Paoletti, Cesaro & Delben, 1983). Collagen triple helices have a high potential for lateral interactions and form a variety of microfibrillar and fibrillar aggregates (Fraser, MacRae & Miller, 1987; van der Rest & Garrone, 1991; Kajava, 1991). The deoxygenated form of sickle-cell hemoglobin molecules polymerize into long strands, and these form dimers by side-by-side association, followed by alignment and lateral aggregation of the dimers to form fibers and macrofibers with specific lateral interactions (Magdoff-Fairchild & Chiu, 1979; Potel, Wellems, Vassar, Deer &

Josephs, 1984). Fibrinogen molecules form two-stranded protofibrils *via* specific lateral interactions, which then aggregate laterally to form fibers (Voter, Lucaveche, Blaurock & Erickson, 1986).

A general expression for the intensity diffracted by a non-crystalline fiber in which the scattering units are made up of a number of identical parallel (or antiparallel) helical molecules is derived, and its computational complexity is assessed. Example calculations using these expressions illustrate the effects of aggregation on diffraction patterns and on the apparent symmetry of the molecules that is inferred from the distribution of diffraction on the meridian of diffraction patterns.

2. Preliminaries

Consider a helical molecule with repeat distance c and helix symmetry u_v, i.e. there are u (helix) repeat units in v turns of the helix (one c repeat). The complex amplitude $F_l(R, \psi)$ diffracted by such a molecule is given by

$$F_l(R, \psi) = \sum_n G_{nl}(R) \exp[in(\psi + \pi/2)], \quad (1)$$

where $(R, \psi, Z = l/c)$ are cylindrical polar coordinates in reciprocal space, l is an integer, and the sum is over all integers n that satisfy the helix selection rule (Cochran, Crick & Vand, 1952)

$$l = up + vn, \quad (2)$$

where p is any integer. The $G_{nl}(R)$ are the complex Fourier–Bessel structure factors (Klug, Crick & Wyckoff, 1958) given by

$$G_{nl}(R) = \sum_j f_j J_n(2\pi Rr_j) \exp[i(-n\varphi_j + 2\pi l z_j/c)], \quad (3)$$

where the sum is over the atoms that have cylindrical polar coordinates (r_j, φ_j, z_j) and scattering factors f_j, in one helix repeat unit, and $J_n(\cdot)$ is the Bessel function of the first kind of order n. A non-crystalline oriented fiber is made up of many parallel molecules that are randomly positioned relative to each other and randomly rotated about their axes. The intensity diffracted by such a fiber is given by

$$I_l(R) = (1/2\pi) \int_0^{2\pi} |F_l(R, \psi)|^2 \, d\psi \quad (4)$$

and substitution of (1) and (3) into (4) gives

$$I_l(R) = \sum_n |G_{nl}(R)|^2. \quad (5)$$

A polycrystalline fiber is made up of randomly positioned and rotated crystallites, within each of which there is perfect crystalline order. The diffracted intensity is then concentrated at the positions of the cylindrically projected reciprocal lattice and is equal to the sum of the intensities $|F_l(R, \psi)|^2$ at the reciprocal-lattice points with the same cylindrical polar radius (Millane, 1988).

3. Diffraction by an aggregate

Consider a non-crystalline fiber in which the diffracting units are aggregates of N helical molecules, formed as a result of specific side-to-side interactions. The molecular axis of the jth molecule intersects the $z = 0$ plane at the point with cylindrical polar coordinates (ρ_j, β_j), and the molecule is rotated about, and shifted along, its local helix axis by α_j and ζ_j, respectively, relative to a reference molecule at the origin. Using (1) and (3) shows that the complex amplitude diffracted by the aggregate is given by

$$F_l(R, \psi) = \sum_j \sum_n G_{nl}(R) \exp[in(\psi - \alpha_j + \pi/2)]$$

$$\times \exp[i2\pi R\rho_j \cos(\psi - \beta_j)] \exp(i2\pi l\zeta_j/c), \quad (6)$$

where the $G_{nl}(R)$ are the Fourier–Bessel structure factors for the reference molecule. Substituting (6) and (4), making some trigonometric simplifications and using the integral form for Bessel functions, one finds that the intensity diffracted by such a fiber is given by

$$I_l(R) = \sum_j \sum_k \sum_m \sum_n G_{ml}(R) G_{nl}^*(R) J_{n-m}(2\pi R\rho_{jk})$$

$$\times \exp\{i[(m - n)\beta_{jk} - m\alpha_j + n\alpha_k + 2\pi l\zeta_{jk}/c]\}. \quad (7)$$

In this equation, the sums over j and k are over the N molecules, the sums over m and n are over the solutions to the helix selection rule (2), $*$ denotes the complex conjugate, ρ_{jk} is the length of the vector joining the points (ρ_j, β_j) and (ρ_k, β_k), β_{jk} is the angle between this vector and the $\varphi = 0$ axis, $\beta_{jj} = 0$ and $\zeta_{jk} = \zeta_j - \zeta_k$. Equation (7) is then a succinct form of the required result. The advantage of (7) over a calculation directly from the aggregate structure is that the $G_{nl}(R)$ are calculated from a single helix repeat unit of a single molecule, rather than from one c repeat of the whole aggregate (since the aggregate generally has no helix symmetry). Furthermore, the selection rule, and the resulting computational savings, do not apply to diffraction by the aggregate itself. The computational advantages of (7) are examined more quantitatively below.

Considerable insight into (7), as well as a reduction in the effort required to compute it, can be obtained by separating various terms, and noting that $\rho_{jk} = \rho_{kj}$, $\beta_{jk} = \beta_{kj} + \pi$, $\zeta_{jk} = -\zeta_{kj}$ and $J_{-n}(x) = (-1)^n J_n(x)$, which, after some manipulation, shows that

$$I_l(R) = N \sum_n |G_{nl}(R)|^2 + 2 \sum_n |G_{nl}(R)|^2 \sum_j \sum_{k>j} J_0(2\pi R\rho_{jk})$$

$$\times \cos(-n\alpha_{jk} + 2\pi l\zeta_{jk}/c)$$

$$+ 2 \sum_m \sum_{n>m} \sum_j \sum_{k>j} J_{m-n}(2\pi R\rho_{jk}) \, \Re\{G_{ml}(R) G_{nl}^*(R)$$

$$\times \exp[i(m - n)\beta_{jk}]$$

$$\times \left(\exp[i(-m\alpha_k + n\alpha_j - 2\pi l\zeta_{jk}/c)] \right.$$

$$\left. + (-1)^{m-n} \exp[i(-m\alpha_j + n\alpha_k + 2\pi l\zeta_{jk}/c)] \right)\} \quad (8)$$

where $\Re\{\cdot\}$ denotes the real part and $\alpha_{jk} = \alpha_j - \alpha_k$. Note that, although the $G_{nl}(R)$ have been defined here, using (3), in terms of an atomic model of the molecule, they can be defined for any (for example, low-resolution) model of a helical molecule, so that (7) and (8) can be used for any such model.

In (8), the first term represents the intensity diffracted by a non-crystalline fiber made up of independent molecules and the remaining two terms (multiple summations) are due to interference effects resulting from the specific geometric relationships between the molecules in an aggregate. The first two terms correspond to an expression derived by Fraser, MacRae & Miller (1964) for the case in which only a single Bessel term n contributes on each layer line. In most cases, however, multiple Bessel terms contribute on each layer line and the third term in (8) must be included. If there are many (in practice, not very many) molecules in the aggregate and there are no special relationships between them (i.e. the ρ_j, β_j, α_j, ζ_j are random), then the terms in the second and third summations in (8) tend to average to zero and only the first term remains. This corresponds to a non-crystalline fiber and (8) reduces to (5). If the aggregate is a crystallite, then the terms in (8) combine to form an interference function that samples the molecular transform at the cylindrically projected reciprocal-lattice points. If there are few molecules in the aggregate, then the effect of the second and third terms is to modulate the intensity that would be diffracted by a non-crystalline fiber of independent molecules.

In the above analysis, each molecule in the aggregate is assumed to be pointing in the same direction. It is not uncommon, however, for biopolymer aggregates to contain molecules that are pointing in both directions, i.e. to contain both 'up' and 'down' molecules. For example, the sickle-cell hemoglobin macrofibers contain up and down dimers, each dimer being made up of side-by-side parallel molecules (Potel, Wellems, Vassar, Deer & Josephs, 1984). The above analysis is therefore extended to accommodate aggregates containing both up and down molecules. Consider an aggregate of N molecules, some of which are up-pointing and the remainder down-pointing. The Fourier–Bessel structure factors and the diffracted complex amplitude for a reference up molecule are given by (3) and (1), respectively. The reference down molecule is defined as the reference up molecule rotated by 180° about the x axis. The Fourier–Bessel structures of the reference down molecule are then $G^*_{nl}(R)$ and the diffracted amplitude is

$$F_l^D(R, \psi) = \sum_n G^*_{nl}(R)\exp[in(\psi + \pi/2)]. \quad (9)$$

An aggregate containing both up and down molecules can be generated by applying appropriate rotations and translations to these reference up and down molecules. Because of the complex conjugate in (9), the expression for the intensity diffracted by the fiber cannot be

factorized as simply as for the case when all the molecules are pointing in the same direction. It is convenient to treat the aggregate as a set of up molecules and a set of down molecules. Calculating the complex amplitudes due to each set, adding, and performing the angular average (4), one obtains the intensity diffracted by the fiber as

$$I_l(R) = I_l^U(R) + I_l^D(R) + I_l^{UD}(R), \quad (10)$$

where $I_l^U(R)$ and $I_l^D(R)$ are the cylindrically averaged intensities diffracted by the set of up and the set of down molecules, respectively. $I_l^U(R)$ is given by (7) [or (8)] and $I_l^D(R)$ is given by (7) [or (8)] with $G_{nl}(R)$ replaced by $G^*_{nl}(R)$. The term $I_l^{UD}(R)$ represents the interference effects between the up and down molecules and is given by

$$I_l^{UD}(R) = 2\sum_j \sum_k \sum_m \sum_n J_{n-m}(2\pi R r_{jk}) \Re\{G_{ml}(R) G_{nl}(R)$$
$$\times \exp\left(i[(m - n)\beta_{jk} - m\alpha_j + n\alpha_k + 2\pi l\zeta_{jk}/c]\right)\} \quad (11)$$

where the sums over j and k are over only the up and only the down molecules, respectively. Use of (10) and (11) offers similar computational savings as described above.

It is informative to examine the computational cost involved in evaluating (7) [or (8)] compared to a direct calculation. As a result of the selection rule and the behavior of Bessel functions, the number of Fourier–Bessel structure factors required at a particular resolution on a particular layer line is approximately proportional to the radius of the molecule and inversely proportional to the helix symmetry u (Makowski, 1982; Millane, 1992). The number of terms required to calculate each Fourier–Bessel structure factor is proportional to the number of atoms, p say, in the helical repeat unit. If the aggregate is treated as a single unit, it has one-fold symmetry, Nup atoms in the repeat unit, and a radius of order $N^{1/2}$ relative to the radius of a single molecule. The computational cost is therefore of order $N^{3/2}up$. From (7), the number of Fourier–Bessel structure factors required is reduced by a factor u, and each is calculated using only p atoms. However, the summations over j and k give an additional order N^2 terms associated with each Fourier–Bessel structure factor so that the overall computational cost is of order N^2p/u. Expression (7) is therefore more efficient than the direct calculation by a factor of order $u^2/N^{1/2}$. For high helix symmetry, this can be quite significant. For example, for an aggregate of ten molecules each with tenfold helix symmetry, use of (7) would reduce the computation required by a factor of about 30.

4. Implications

Aside from the computational advantages afforded by the use of (8), this equation can also be used to examine the

effects of aggregation on fiber diffraction patterns. Two aspects are examined here. The first is to assess the effect of the second and third multiple summations in (8) relative to the first term. There are a number of practical implications of this. If these additional terms are small relative to the first, then the fact that the molecules form aggregates may not be apparent in the diffraction data. This would be an advantage if one wishes to determine only the structure of a single molecule from the diffraction data, since the effects of aggregation would not distort the analysis. However, it would be a disadvantage if one is interested in if, and how, the molecules aggregate, because the data containing this information may be below the noise level. Also, since the transform of a single helical molecule is zero on the meridian of all layer lines except those for which $l = mu$ where m is an integer, the helix symmetry of a molecule is usually determined from a fiber diffraction pattern by inspection of the systematic absences along the meridian. Certain types of aggregation can affect the relationship between the helix symmetry and the pattern of meridional reflections and thus the determination of the helix symmetry of the molecules. These aspects are explored here by calculating diffraction patterns for aggregates (dimers) made up of two molecules. For a dimer, we can set $\rho_1 = \beta_1 = \alpha_1 = \zeta_1 = \beta_2 = 0$ and use the convention $\rho_2 = \rho$, $\alpha_2 = \alpha$, $\zeta_2 = \zeta$. In this case, (8) reduces to

$$I_l(R) = 2\sum_n |G_{nl}(R)|^2 [1 + J_0(2\pi R\rho)\cos(n\alpha - 2\pi l\zeta/c)]$$
$$+ 2\sum_m \sum_{n>m} J_{m-n}(2\pi R\rho) \, \Re\{G_{ml}(R) G^*_{nl}(R)$$
$$\times \left(\exp[i(-m\alpha + 2\pi l\zeta/c)] \right.$$
$$\left. + (-1)^{m-n} \exp[i(n\alpha - 2\pi l\zeta/c)]\}\right). \qquad (12)$$

Example diffraction patterns are calculated using (12) and using the asymmetric unit of κ-carrageenan (Millane, Chandrasekaran, Arnott & Dea, 1988) as the helix repeat unit. The radius of the molecules generated is ca 7.5 Å.

The intensities diffracted by dimers containing molecules with 2_1 and 5_1 helix symmetry are shown as the solid lines in Fig. 1 and can be compared with the diffraction from single molecules (broken lines). The effect of the aggregation is to modulate the amplitude diffracted by a single molecule. The main differences between the two are at low resolution, where the diffraction reflects the overall size of the dimer compared to that of the single molecule. Elsewhere, particularly at higher resolution, the differences are rather small. The effects tend to be more significant for lower than for higher helix symmetry. The relative r.m.s. difference between the amplitudes diffracted by the dimer and by a single molecule, between 20 and 3 Å resolution, is only about 10% for the examples shown in Fig. 1. In these examples, the formation of an aggregate might be detectable in the diffraction pattern from the 2_1 molecule,

but probably not in the case of the 5_1 molecule. The differences may be more noticeable, however, if there are special relationships between the molecules, as is shown below. For more than two molecules, the interference effects will be even less significant unless there are special geometrical relationships between the molecules (in which case the modulation would be more structured). Overall, these results indicate that aggregation of even only a few molecules should not seriously affect interpretation of diffraction patterns in terms of the structure of a single molecule.

It is quite common for molecules to aggregate such that the axial shift (or 'stagger') is an integral fraction of the c repeat. This case is examined here for 'half-staggered' dimers, for which $\zeta = c/2$ and $\alpha = 0$.
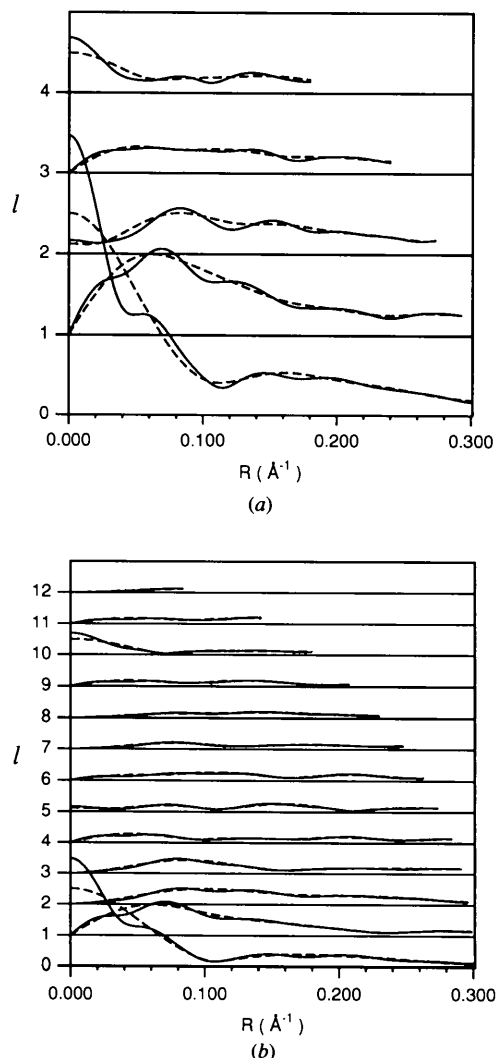

Fig. 1. Amplitude diffracted by helical molecules with (a) 2_1 and (b) 5_1 helix symmetry (- - -), and by dimers made up of two such molecules (———). In these simulations, $\rho = 15$ Å and $\alpha = \zeta = 0$.

Equation (12) then reduces to

$$I_l(R) = 2 \sum_n |G_{nl}(R)|^2 [1 + (-1)^l J_0(2\pi R\rho)]$$

$$+ 2 \sum_m \sum_{n>m} J_{m-n}(2\pi R\rho) \, \Re\{G_{ml}(R) \, G_{nl}^*(R)$$

$$\times (-1)^l [1 + (-1)^{m-n}]\}. \tag{13}$$

If the two molecules are co-axial, then $\rho = 0$ and (13) reduces to

$$I_l(R) = 4 \sum_n |G_{nl}(R)|^2, \quad l \text{ even}$$
$$= 0, \qquad\qquad l \text{ odd}. \tag{14}$$

This is a familiar case and the layer-line spacing is doubled, reflecting the halving of the c repeat of the

Fig. 2. Amplitude diffracted by helical molecules with (a) 4_1 and (b) 3_1 helix symmetry (- - -), and by non-co-axial half-staggered dimers made up of two such molecules with $\rho = 15$ Å (———).

Table 1. *Apparent helix symmetry (based on the distribution of meridional reflections) of co-axial and non-co-axial dimers containing u-fold helical molecules*

u	Co-axial	Non-co-axial
Odd	u	$2u$
Even	$u/2$	u

dimer relative to that of a single molecule. The effect on the distribution of meridional intensity is rather easy to see. The co-axial dimer can be treated as a single helical molecule and the pattern of meridional reflections corresponds to the helix symmetry of the dimer. The helix symmetry of the co-axial dimer is equal to u if u is odd and to $u/2$ if u is even, where u is the helix symmetry of the constituent molecules.

If the half-staggered dimer is not co-axial, then the c repeat and the layer-line spacing are the same as for a single molecule. Inspection of (13) shows that (14) then applies only if $R = 0$, *i.e.* only on the meridian. The dimer itself has only onefold helix symmetry (*i.e.* no symmetry). From (14), if u is even, the meridional reflections are present on every uth layer line, which corresponds to the helix symmetry of the constituent molecules. If u is odd, however, then some of the meridional reflections are eliminated and the remainder are on every $2u$th layer line, which corresponds to the helix symmetry of neither the constituent molecules nor the dimer. This is summarized in Table 1 and is illustrated in Fig. 2 for molecules with 4_1 and 3_1 helix symmetry. Note that in Fig. 2(b) the first meridional reflection for the dimer is on the sixth layer line, although the constituent molecules have threefold symmetry. Hence, in such cases, one has to be careful when interpreting the pattern of meridional reflections in terms of the helix symmetry of the molecules.
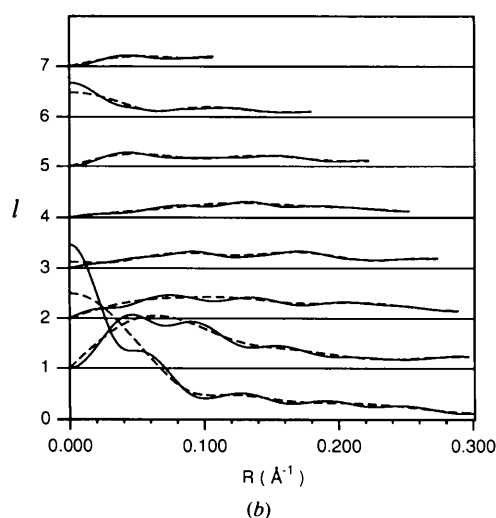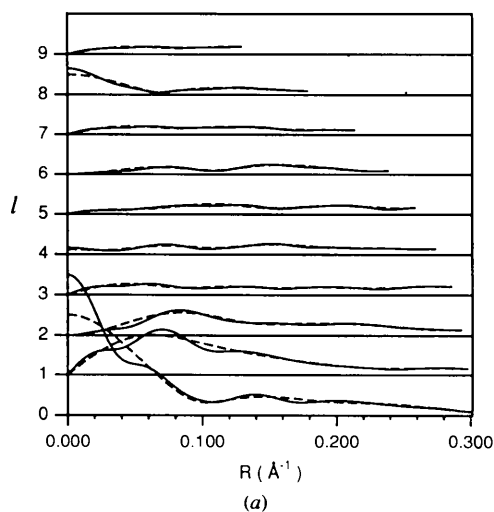
5. Concluding remarks

An expression has been derived for the intensity diffracted by a non-crystalline fiber made up of aggregates of identical parallel (or antiparallel) helical molecules. This expression allows the effects of aggregation to be evaluated and leads to computational advantages compared to a calculation directly from the aggregate structure. Example calculations show that the effects of aggregation on fiber diffraction patterns are often rather small, which has implications for structure determination. Aggregates in which the molecules are non-co-axial, but staggered in a particular way, can lead to unexpected relationships between the helix symmetry and the distribution of meridional reflections.

References

BHATTACHARJEE, S., GLUCKSMAN, M. J. & MAKOWSKI, L. (1992). *Biophys. J.* **61**, 725–735.

CHANDRASEKARAN, R., MILLANE, R. P., ARNOTT, S. & ATKINS, E. D. T. (1988). *Carbohydr. Res.* **175**, 1–15.

COCHRAN, W., CRICK, F. H. C. & VAND, V. (1952). *Acta Cryst.* **5**, 581–586.

FRASER, R. D. B., MACRAE, T. P. & MILLER, A. (1964). *Acta Cryst.* **17**, 769–770.

FRASER, R. D. B., MACRAE, T. P. & MILLER, A. (1987). *J. Mol. Biol.* **193**, 115–125.

KAJAVA, A. V. (1991). *J. Mol. Biol.* **218**, 815–823.

KLUG, A., CRICK, F. H. C. & WYCKOFF, H. W. (1958). *Acta Cryst.* **11**, 199–213.

LESLIE, A. G. W., ARNOTT, A., CHANDRASEKARAN, R. & RATLIFF, R. L. (1980). *J. Mol. Biol.* **143**, 49–72.

MAGDOFF-FAIRCHILD, B. & CHIU, C. C. (1979). *Proc. Natl Acad. Sci. USA*, **76**, 223–226.

MAKOWSKI, L. (1982). *J. Appl. Cryst.* **15**, 546–557.

MILLANE, R. P. (1988). *Crystallographic Computing 4. Techniques and New Technologies*, edited by N. W. ISAACS & M. R. TAYLOR, pp. 169–186. IUCr/Oxford Univ. Press.

MILLANE, R. P. (1992). *Acta Cryst.* A**48**, 209–215.

MILLANE, R. P., CHANDRASEKARAN, R., ARNOTT, S. & DEA, I. C. M. (1988). *Carbohydr. Res.* **182**, 1–17.

MILLANE, R. P. & STROUD, W. J. (1991). *Int. J. Biol. Macromol.* **13**, 202–208.

NAMBA, K. & STUBBS, G. J. (1985). *Acta Cryst.* A**41**, 252–262.

PAOLETTI, S., CESARO, A. & DELBEN, F. (1983). *Carbohydr. Res.* **123**, 173–178.

PARK, H. S., ARNOTT, A., CHANDRASEKARAN, R., MILLANE, R. P. & CAMPAGNARI, F. (1987). *J. Mol. Biol.* **197**, 513–523.

POTEL, M. J., WELLEMS, T. E., VASSAR, R. J., DEER, B. & JOSEPHS, R. (1984). *J. Mol. Biol.* **177**, 819–839.

REST, M. VAN DER & GARRONE, R. (1991). *FASEB J.* **5**, 2814–2823.

VOTER, W. A., LUCAVECHE, C., BLAUROCK, A. E. & ERICKSON, H. P. (1986). *Biopolymers*, **25**, 2359–2373.

Orientational Order and Disorder in Solid C60: Theory and Diffraction Experiments

BY K. H. MICHEL

Department of Physics, Universiteit Antwerpen (UIA), 2610 Wilrijk, Belgium

D. LAMOEN

Max-Planck-Institut für Festkörperforschung, Postfach 800665, 70506 Stuttgart, Germany

AND W. I. F. DAVID

ISIS Science Division, Rutherford Appleton Laboratory, Chilton, Didcot, Oxon OX11 0QX, England

Abstract

Starting from a microscope model of the intermolecular potential, a unified description is presented of the Bragg scattering law in the orientationally disordered and in the ordered phase of solid C_{60}. The orientational structure factor is expanded in terms of symmetry-adapted surface harmonics. The expansion coefficients are calculated from theory and compared with experiment. Their temperature evolution is studied in the disordered phase at the 260 K transitions and in the ordered phase. In the ordered phase, new results from high-resolution neutron powder diffraction are given. In the disordered phase, space group $Fm\bar{3}m$, the reflections have A_{1g} symmetry; in the ordered phase, space group $Pa\bar{3}$, reflections of T_{2g} symmetry appear and in addition the A_{1g} reflections are renormalized. The orientational density distribution is calculated. The effective crystal-field potential is constructed, its temperature evolution in the ordered phase is studied and related to the occurrence of an orientational glass.

1. Introduction

C_{60}-fullerite is a molecular crystal (Krätschmer, Lamb, Fostiropoulos & Huffman, 1990). At room temperature, the space group is $Fm\bar{3}m$ (Fleming *et al.*, 1991) and the molecules are orientationally disordered. At a transition temperature $T_1 \simeq 260$ K, the crystal undergoes a phase change (Dworkin *et al.*, 1991; Heiney *et al.*, 1991a) to a $Pa\bar{3}$ structure (Sachidanandam & Harris, 1991; Heiney *et al.*, 1991b; David *et al.*, 1991). The molecules are orientationally ordered on four different sublattices (Harris & Sachidanandam, 1992). Neutron powder diffraction (David *et al.*, 1991) and single-crystal X-ray studies (Liu, Lu, Kappes & Ibers, 1991; Bürgi *et al.*, 1992) of the low-temperature ordered structure have revealed the packing configuration of the C_{60} molecules. In an optimized ordering scheme, electron-rich double bonds that fuse the hexagons on the C_{60} molecule face pentagons of adjacent C_{60} units. This idea has been implemented in molecular dynamics calculations (Sprik, Cheng & Klein, 1992). A theoretical description of the